STRUCTURE AND PROPERTIES OF MELT-SPUN Al-Zr-Ti ALLOYS IV. MICROSTRUCTURE AND MICROHARDNESS STABILITY AT ELEVATED TEMPERATURES

PŘEMYSL MÁLEK, MILOŠ JANEČEK, BOHUMIL SMOLA

The influence of long term annealing at temperatures up to 773 K on microhardness and the microstructure of several melt spun Al-Zr-Ti alloys was studied. The microhardness stability depends on the content of Zr and Ti in these alloys. The best results were obtained in the Al-$Al_3(Zr_{0.5}Ti_{0.5})$ alloy where microhardness increases during annealing at 600 K with time up to 500 hours. The peak microhardness corresponds to the microstructure containing very small particles of the metastable $L1_2$ $Al_3(Zr_xTi_{1-x})$ phase formed by discontinuous precipitation. Over-aging occurring for longer annealing times at temperatures $T \geq 650$ K is caused by the formation of much coarser particles of the stable $Al_3(Zr_xTi_{1-x})$ phase. The difference between the decomposition behaviour of supersaturated Zr-rich and Ti-rich Al-Zr-Ti alloys may be explained as a result of extremely different diffusion rates of Zr and Ti in Al at temperatures close to 600 K.

Key words: Al-based alloys for elevated temperatures, rapid solidification, microstructure, transmission electron microscopy, microhardness, elevated temperature stability

STRUKTURA A VLASTNOSTI SLITIN Al-Zr-Ti PŘIPRAVENÝCH METODOU „MELT SPINNING" IV. STABILITA MIKROSTRUKTURY A MIKROTVRDOSTI U ZVÝŠENÝCH TEPLOT

V práci byl studován vliv dlouhodobého žíhání u teplot až do 773 K na mikrostrukturu a mikrotvrdost slitin Al-Zr-Ti připravených metodou melt spinning. Stabilita mikrotvrdosti závisí na obsahu Zr a Ti v těchto slitinách. Nejlepší výsledky byly dosaženy u slitiny Al-$Al_3(Zr_{0,5}Ti_{0,5})$, jejíž mikrotvrdost dokonce roste během žíhání po dobu až 500 hodin u teploty 600 K. Maximální mikrotvrdost odpovídá mikrostruktuře obsahující velmi jemné částice metastabilní $L1_2$ $Al_3(Zr_xTi_{1-x})$ fáze precipitující diskontinuálně. Přestárnutí pozorované pro delší doby žíhání u teplot $T \geq 650$ K je důsledkem tvorby mno-

RNDr. P. Málek, CSc., RNDr. M. Janeček, CSc., Doc. RNDr. B. Smola, CSc., Department of Metal Physics, Charles University, Ke Karlovu 5, 121 16 Prague 2, Czech Republic.

hem hrubších částic stabilní fáze $Al_3(Zr_xTi_{1-x})$. Rozdíly v rozpadu přesycených slitin bohatých na Zr, resp. bohatých na Ti mohou být vysvětleny jako důsledek extrémně odlišných rychlostí difuze Zr a Ti atomů v Al u teplot kolem 600 K.

1. Introduction

New aluminium-based alloys are developed for elevated temperature applications. Their improved microstructure and strength stability at elevated temperatures is achieved by preventing the dissolution and coarsening of strengthening dispersion particles or precipitates. Many recent investigations have revealed that the Al-Zr system may be a good basis for the development of such alloys if they are prepared using rapid solidification techniques (e.g. [1–5]). Particles of the Al_3Zr phase which are formed either during solidification or during the decomposition of the supersaturated rapidly solidified material contribute to the strengthening. These particles resist well to dissolution at elevated temperatures due to a slight temperature dependence of the solid solubility of Zr in Al [6] and, therefore, their volume fraction remains high up to the melting point. The stability of their small size is then the main problem which is involved.

Previous experiments revealed [4, 7–9] that a partial substitution of Zr atoms by ternary elements (e.g. V, Ti or Hf) may modify the lattice parameters of the Al_3Zr-based phase and reduce its lattice mismatch to the Al matrix. The Al-Zr--Ti system was chosen for our experiments. Chemically homogeneous, fine grained samples of these alloys were prepared using the melt spinning method [10]. Both the microstructure and the phase composition are influenced by the substitution of Ti for Zr atoms [11]. The Zr-rich alloys are not single phase materials and the metastable $Al_3(Zr_xTi_{1-x})$ phase with the cubic $L1_2$ structure was found in the as melt-spun state. Very fine particles of this phase are usually arranged into fans. The measurement of the lattice parameter of this phase confirmed unambiguously that Ti atoms replaced the Zr ones in the lattice of this phase and the lattice misfit decreased to zero for the stoichiometric parameter close to 0.75. The tendency to the formation of fans of fine particles decreases in the Ti-rich alloys where individual coarse particles (containing probably Fe) prevail [11]. Microhardness values measured in the as-melt-spun Al-Zr-Ti alloys exhibit a significant scatter. Much higher values obtained in the Zr-rich alloys suggest that the $Al_3(Zr_xTi_{1-x})$ phase particles are the most important obstacles contributing to a high strength.

The coarsening of strengthening particles is generally believed to be the main process controlling the strength at elevated temperatures. However, our investigation of the decomposition of Al-Zr-Ti alloys revealed that the metastable $L1_2$ $Al_3(Zr_xTi_{1-x})$ phase is gradually replaced by the stable modification of the $Al_3(Zr_xTi_{1-x})$ phase (DO_{23} and DO_{22} structure in the Zr-rich and in the Ti-rich alloys, respectively) at elevated temperatures. The transition temperature is influenced by the Ti-content. As the lattice mismatch of both stable modifications

is significantly higher in comparison with the metastable modification [6, 12–14], much coarser particle size of the stable $Al_3(Zr_xTi_{1-x})$ phase may be expected. Consequently, a strength drop may be expected at such annealing conditions when the stable modification of the $Al_3(Zr_xTi_{1-x})$ phase is formed. In order to verify this idea, the Al-Zr-Ti alloys were annealed, their microhardness was measured and compared with the results of the microstructure investigation.

2. Material and procedure

The thin Al-Zr-Ti ribbons were prepared using the melt spinning method (for details see [10]). The nominal chemical compositions, which should correspond at room temperature to the equilibrium phase composition of Al–5 vol.% $Al_3(Zr_xTi_{1-x})$ with stoichiometric parameters $x = 1$, 0.75, 0.5, 0.25, and 0 (Table 1), were chosen. The actual chemical compositions were found close to the nominal values [10].

Table 1. Nominal chemical composition of the Al-$Al_3(Zr_xTi_{1-x})$ alloys in wt.%

x	1	0.75	0.5	0.25	0
Zr	4.1	3.1	2.1	1.0	–
Ti	–	0.55	1.1	1.65	2.2

The as-melt-spun Al-Zr-Ti ribbons were annealed under argon protective atmosphere for various times up to 500 hours at temperatures up to 773 K. The annealed samples were mounted into special holders, fixed and polished mechanically. The Knoop microhardness HK was measured on the polished longitudinal sections of ribbons at room temperature with the load of 10 g and the dwell time of 15 s. The indents were applied close to the centre of the ribbon. At least 15 measurements were carried out on each sample.

The internal microstructure of annealed samples was studied using the transmission electron microscopy. The ribbons were thinned electrolytically in the 66%HNO_3–33%CH_3OH solution. The observations were carried out in an electron microscope JEOL 2000 FX at 200 kV. Electron diffraction experiments were performed in order to identify the structure of particles.

3. Experimental results

Electrical resistance measurements revealed that the metastable as-melt-spun ribbons of all Zr-containing Al-Zr-Ti alloys decomposed at elevated temperatures in two stages. In the binary Al-Zr alloy the first stage started at about 550 K and

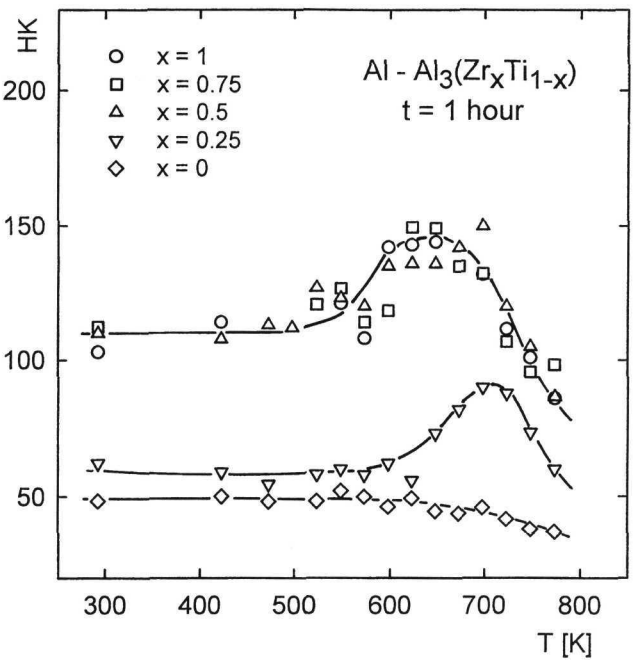

Fig. 1. Isochronal annealing curves of microhardness for different Al-Zr-Ti alloys.

the second stage at about 670 K. Both stages were shifted to higher temperatures if Zr atoms were partially replaced by Ti ones [15]. The isochronal annealing curves of microhardness for the annealing time of 1 hour (Fig. 1) show a good correlation with the above-mentioned temperature dependence of electrical resistance. An increase in HK was found between about 500 and 650 K in all Zr-rich Al-Zr-Ti alloys ($x \geq 0.5$), i.e. at the temperature where the first stage of decomposition occurs. The expected shift of the HK increase to higher temperatures with decreasing stoichiometric parameter x was not observed in the Zr-rich alloys, especially because of a large scatter of HK values (up to 20%) obtained at temperatures below 550 K. This large scatter reflects the fact that individual samples are partially decomposed already in the as-melt-spun state and the degree of this decomposition is not homogeneous even within each sample. A sharp drop in microhardness starts at temperatures slightly below 700 K in all Zr-rich Al-Zr-Ti alloys. This temperature corresponds well with the onset of the second stage of decomposition. A distinct shift of the microhardness maximum to higher temperatures was found in the Ti-rich Al-Zr-Ti alloy ($x = 0.25$). The maximum value of HK is, however, much lower

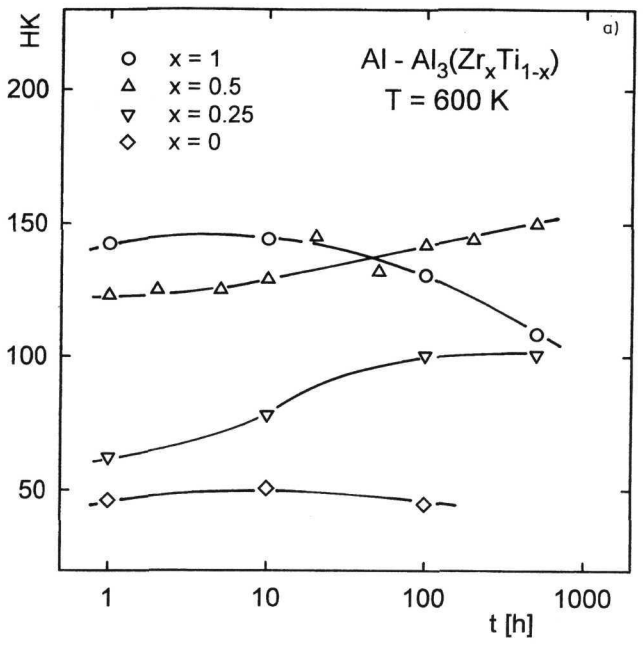
a)
HK
200
150
100
50
x = 1
x = 0.5
x = 0.25
x = 0
Al - Al3(ZrxTi1-x)
T = 600 K
1
10
100
1000
t [h]

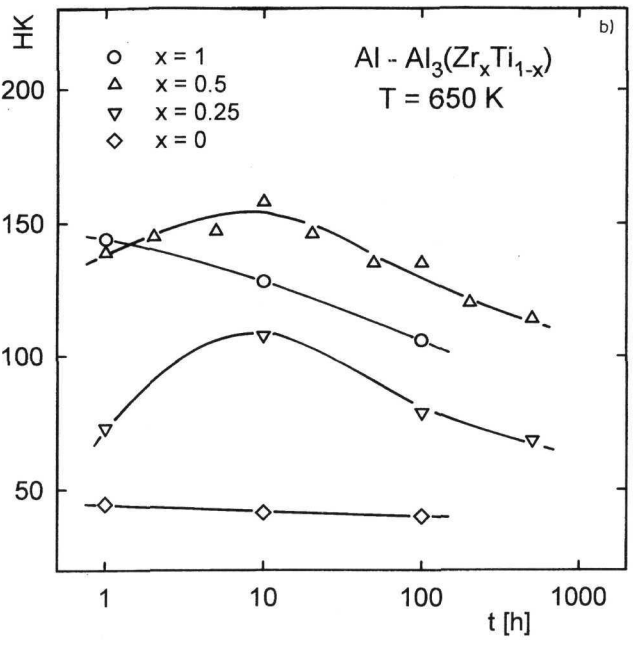
b)
HK
200
150
100
50
x = 1
x = 0.5
x = 0.25
x = 0
Al - Al3(ZrxTi1-x)
T = 650 K
1
10
100
1000
t [h]

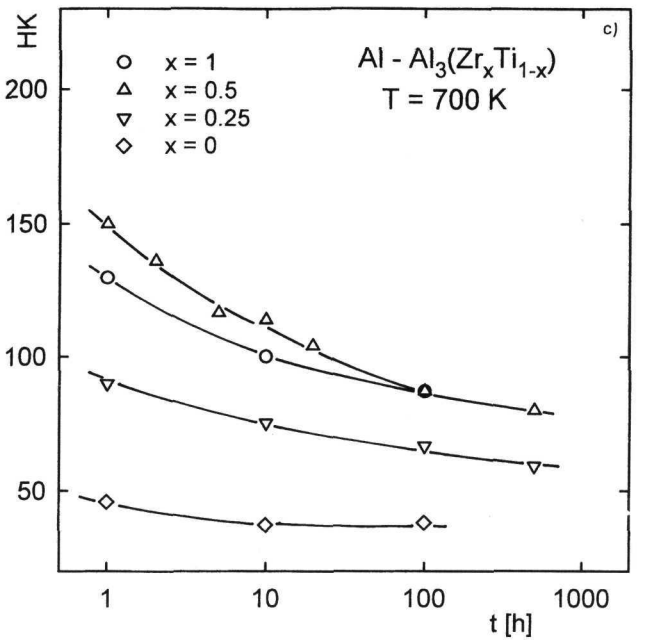

Fig. 2. Isothermal annealing curves of microhardness for different Al-Zr-Ti alloys: a) $T = 600$ K, b) $T = 650$ K, c) $T = 700$ K.

than in the Zr-rich Al-Zr-Ti alloys. No strengthening effect was observed in the binary Al-Ti alloy.

In order to obtain information on the long term stability, the isothermal annealing curves of microhardness were measured at all Al-Zr-Ti alloys in the temperature range between 600 and 700 K (Fig. 2). As the values obtained at the alloy with $x = 0.75$ are very close to those measured at the alloy with $x = 0.5$, only the latter values are plotted in Fig. 2. Several important conclusions may be drawn from this experiment.

– The binary Al-Zr alloy does not retain its high microhardness even during annealing at the lowest temperature of 600 K and a decrease in HK starts after about 10 hours of annealing. The increase in the annealing temperature accelerates the softening process.

– The Zr-rich Al-Zr-Ti alloy with $x = 0.5$ is much more stable than the binary Al-Zr alloy. The maximum of microhardness was not reached at 600 K for annealing times up to 500 hours. The strengthening effect was observed also at 650 K for annealing times up to 10 hours. Despite of the softening occurring at longer annealing times, the HK values remain higher than those in the Al-Zr alloy. The

annealing temperature of 700 K seems to be too high, and the alloy softens for annealing times longer than 1 hour.

– The Ti-rich Al-Zr-Ti alloy with $x = 0.25$ exhibits a similar stability as the alloy with $x = 0.5$, however, the microhardness values are significantly lower than those measured at the Zr-rich alloys.

– The binary Al-Ti alloy does not exhibit any strengthening and its microhardness is deeply below values measured even in the alloy with $x = 0.25$.

Using the results of X-ray diffraction experiments the first stage of decomposition of Zr-rich Al-Zr-Ti alloys was explained by the formation of the metastable $L1_2$ $Al_3(Zr_xTi_{1-x})$ phase and the second stage by the formation of the stable DO_{23} $Al_3(Zr_xTi_{1-x})$ phase. An attempt was made to correlate the microhardness changes directly with these phase composition changes. The pairs of annealing time t and temperature T which correspond to the maxima of isothermal annealing curves of microhardness were plotted in Fig. 3a. At some temperatures the annealing times corresponding to the microhardness maximum could not be exactly determined as the maxima were located out of the range of annealing times used. In this case either the minimum or the maximum annealing times used in our experiments were plotted in Fig. 3a and marked by arrows directed either to the left or to the right. The curves plotted in Fig. 3a divide the $t - T$ space into two regions – the region of strengthening below the curve and the region of softening above the curve. Fig. 3a shows that a partial substitution of Ti for Zr shifts this border curve to higher T or longer t and improves, thus, the elevated temperature stability of Al-Zr-Ti alloys. The curves plotted in Fig. 3b were constructed on the basis of X-ray diffraction experiments [15] and divide the $t-T$ space into two regions – the region where only $L1_2$ modification of the $Al_3(Zr_xTi_{1-x})$ phase was detected (below the curves) and the region where the stable modification of the $Al_3(Zr_xTi_{1-x})$ phase was also present (above the curves), respectively. The comparison of Figs. 3a and 3b shows that the softening of Zr-rich Al-Zr-Ti alloys is probably connected with the formation of the stable $Al_3(Zr_xTi_{1-x})$ phase.

The strength of particle strengthened alloys increases generally with increasing volume fraction of particles and decreases with increasing particle size. Both these structural parameters may be investigated using TEM experiments. The results of other experimental methods reported previously [10, 11, 15] suggest that the Al-Zr-Ti alloys may be divided into two groups – the Zr-rich alloys ($x \geq 0.5$) and the Ti-rich alloys ($x \leq 0.25$). The properties of alloys which belong to individual groups are very similar. The TEM investigation confirms this division.

The presence of particles of the metastable $Al_3(Zr_xTi_{1-x})$ phase already in the as-melt-spun state is a typical structural feature of the Zr-rich Al-Zr-Ti alloys. These particles appear either in a fan-shaped morphology or as slightly coarser individual particles [11]. Fig. 4 shows the presence of such fans in nearly all grains of the binary Al-Zr alloy annealed to the peak microhardness ($T = 600$ K, $t = 10$

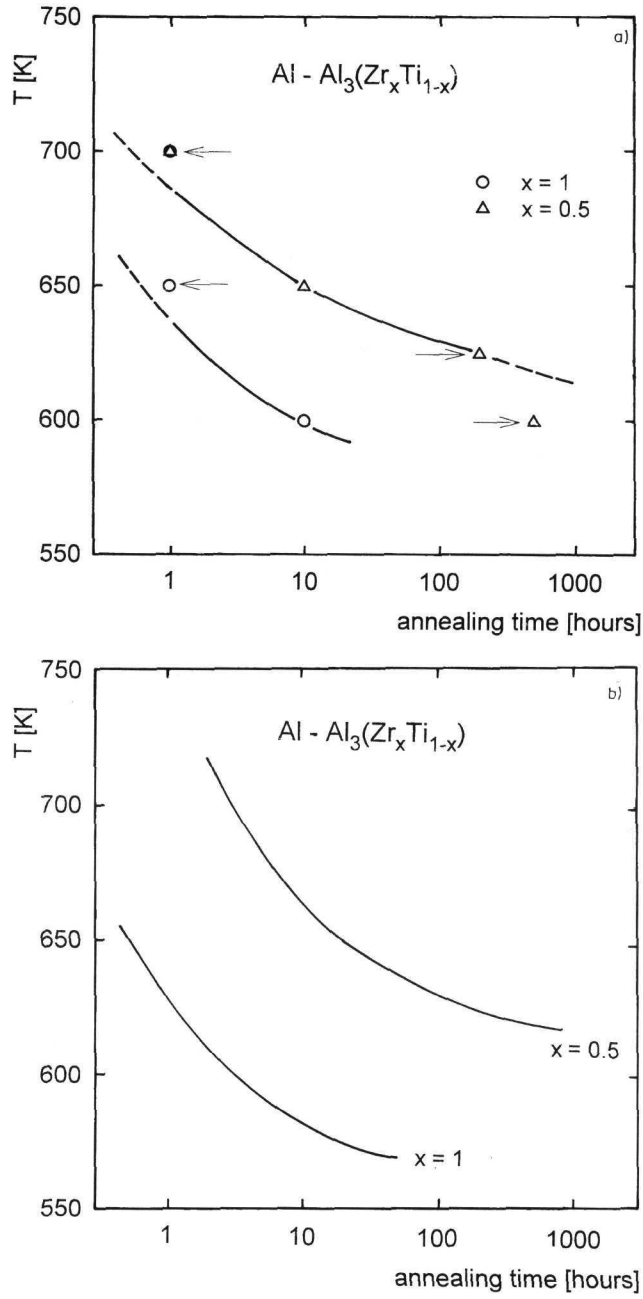

Fig. 3. The transformation diagrams: a) the onset of the microhardness decrease, b) the onset of the formation of the stable $D0_{23}$ $Al_3(Zr_xTi_{1-x})$ phase.

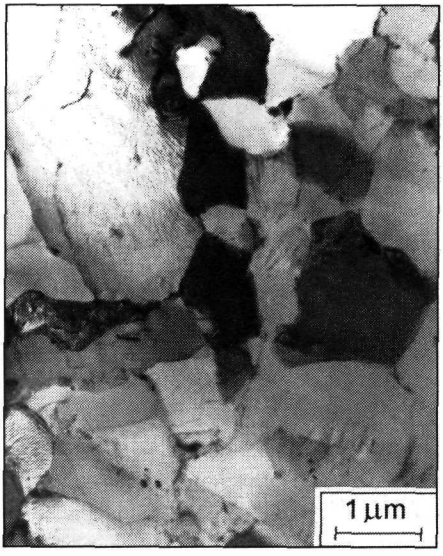

Fig. 4. Microstructure of the peak-aged binary Al-Zr alloy, $T = 600$ K, $t = 10$ hours.

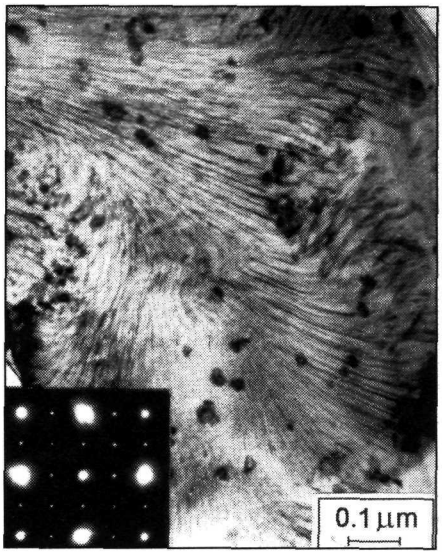

Fig. 5. Microstructure of the peak-aged Zr-rich Al-Zr-Ti alloy ($x = 0.5$), $T = 600$ K, $t = 500$ hours.

hours). The same microstructure was observed also in the peak annealed Al-Zr-Ti alloy with $x = 0.5$ (Fig. 5). The fans consist of very small particles (diameter below 10 nm) which were identified using the electron diffraction analysis as coherent particles of the metastable $Al_3(Zr_xTi_{1-x})$ phase with the $L1_2$ structure in the "cube to cube" orientation relationship to the matrix. Individual slightly coarser incoherent particles of the same phase may be also found between the fan arms. The increase in the annealing temperature to 650 K results at long annealing times in the coarsening and partial dissolution of fans, especially in the vicinity of grain boundaries, and also in the coarsening of the individual particles of the metastable $Al_3(Zr_xTi_{1-x})$ phase (Fig. 6). The formation of coarse particles with the size of about 100 nm was observed during long term annealing at 650 K. These particles were identified as the stable $Al_3(Zr_xTi_{1-x})$ phase with the DO_{23} structure. The number of these coarse particles increased significantly in the sample of the Al-Zr--Ti alloy with $x = 0.5$ annealed at 700 K (Fig. 7). On the other hand, the fans of particles of the metastable $Al_3(Zr_xTi_{1-x})$ phase survive only in a very limited number of grains.

It was reported previously [10] that the microstructure of the Ti-rich Al-Zr-Ti alloys is different already in the as-melt-spun state. They contain predominantly

Fig. 6. Microstructure of the slightly over-aged Zr-rich Al-Zr-Ti alloy ($x = 0.5$), $T =$ 650 K, $t = 500$ hours.

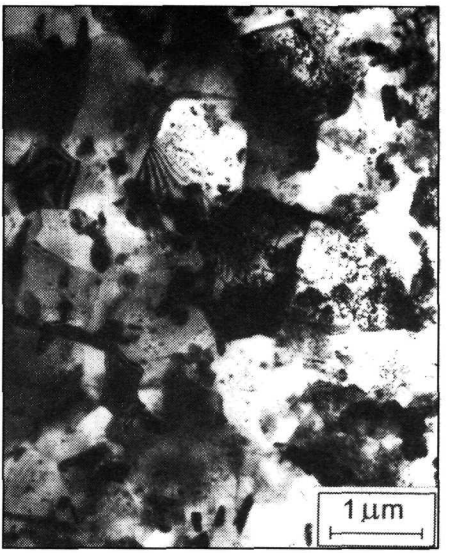

Fig. 7. Microstructure of the severely over-aged Zr-rich Al-Zr-Ti alloy ($x = 0.5$), $T =$ 700 K, $t = 500$ hours.

individual particles and the fan shaped arrangement of particles was observed only in a very limited number of grains of the alloy with $x = 0.25$. The Ti-rich Al-Zr-Ti alloys exhibit also a different structure evolution during annealing. The annealing of the Al-Zr-Ti alloy with $x = 0.25$ to the peak microhardness results in the precipitation of numerous small individual particles of the metastable $Al_3(Zr_xTi_{1-x})$ phase. These particles are concentrated especially at the grain centres, and precipitate free zones are formed along grain boundaries (Fig. 8a). The fan shaped morphology was observed only in a limited number of grains even at the peak microhardness conditions (Fig. 8b). The structure of the Al-Zr-Ti alloy with $x = 0.25$ annealed for a long time at 700 K reveals further concentration of small particles near the grain centres and the dissolution of particle fans (Fig. 9a). Numerous coarse particles with the size exceeding 100 nm were found both at grain boundaries and in grain interiors (Fig. 9b). The electron diffraction analysis failed to determine the crystallographic structure of these particles. The presence of Fe and Si in many of these particles proved by means of EDX analysis suggests that these particles are formed by complex phases. A similar microstructure was found also in the binary Al-Ti alloy annealed at 700 K (Fig. 10).

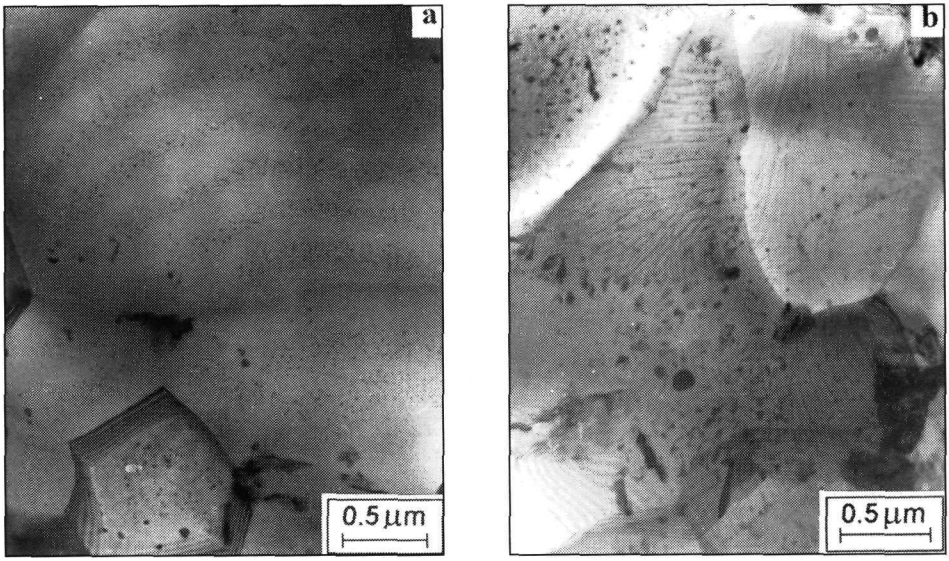

Fig. 8. Microstructure of the peak-aged Ti-rich Al-Zr-Ti alloy ($x = 0.25$), $T = 600$ K, $t = 100$ hours: a) continuous precipitation, b) discontinuous precipitation.

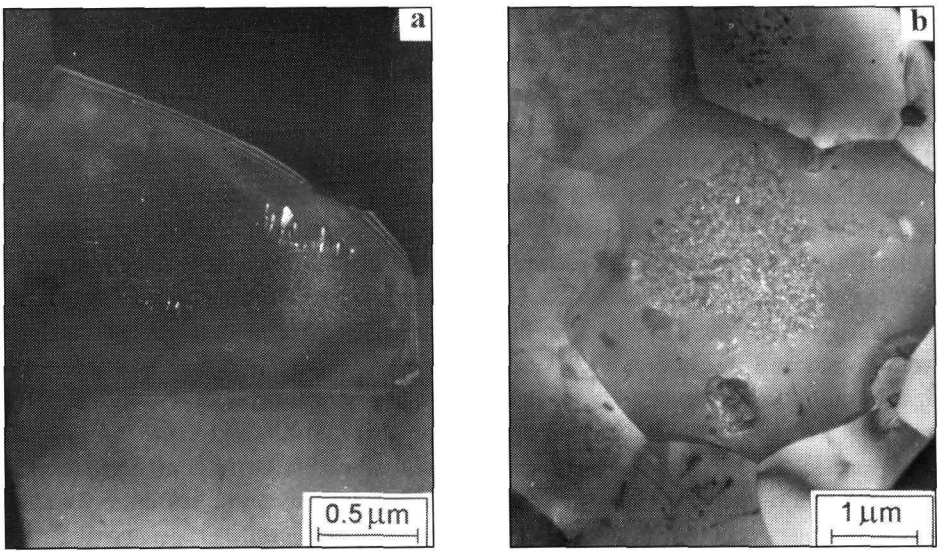

Fig. 9. Microstructure of the over-aged Ti-rich Al-Zr-Ti alloy ($x = 0.25$), $T = 700$ K: a) $t = 100$ hours, dark field, b) $t = 500$ hours.

4. Discussion

Microhardness measurement is the only experimental method which may be used to characterise the strength of very thin melt-spun ribbons. Knoop microhardness values found in the Al-Zr-Ti alloys studied range from about 40 to 150 and reflect the phase composition of individual samples. The phase composition inhomogeneity even within individual samples is probably the reason for the significant scatter in HK values (up to 20%), especially in the Zr-rich Al-Zr-Ti alloys annealed at temperatures below about 573 K.

Fig. 10. Microstructure of the annealed Al-Ti alloy, $T = 700$ K, $t = 100$ hours.

All the Zr-containing materials studied exhibit age-hardening response if annealed at temperatures between about 573 and 673 K. This behaviour is a consequence of the decomposition of the supersaturated matrix which was previously revealed, especially using electrical resistance measurements and X-ray diffraction analysis [15]. The rate of this age-hardening depends significantly on the chemical composition and decreases generally with decreasing Zr content. This effect is well documented in Fig. 3a which shows that the maximum of microhardness is shifted to higher annealing temperatures and longer annealing times in the Al-$Al_3(Zr_{0.5}Ti_{0.5})$ alloy in comparison with the Al-Al_3Zr alloy. This shift agrees well with the results of electrical resistance measurements and X-ray diffraction analysis [15]. The maximum microhardness is observed at such annealing conditions when the maximum density of fans consisting of small particles of the metastable $L1_2$ modification of the $Al_3(Zr_xTi_{1-x})$ phase is achieved.

Over-ageing occurring beyond the microhardness peak was observed in all Zr-containing alloys studied. The onset of this process depends on the Zr content. The comparison with the results of X-ray diffraction analysis [15] and TEM investigations shows that over-ageing occurs at such annealing conditions when the stable modification of the $Al_3(Zr_xTi_{1-x})$ phase starts to form and to replace gradually the metastable one. Much larger size of the stable $Al_3(Zr_xTi_{1-x})$ particles is the main reason for the microhardness decrease.

The maximum microhardness values close to $HK = 150$ which were observed in the Zr-rich Al-Zr-Ti alloys can be compared with some literature data. Microhardness values of conventional age-hardenable Al-based alloys lie usually between 150 and 200 [16], i.e. slightly above the value achieved in our materials. However, the main advantage of our Zr-rich Al-Zr-Ti alloys is that their high microhardness is reasonably stable during annealing at the temperature of 600 K whereas the microhardness of conventional Al-based alloys decreases already at about 450 K. Sahin and Jones [2] measured the isochronal annealing curves of Vickers microhardness of several rapidly solidified binary Al-Zr alloys (annealing time of 1 hour) and reported an increase in HV with increasing Zr content. The alloy containing 1.2 at.% Zr (this composition is very close to our alloys) exhibited the peak value of $HV = 140$ after annealing at 623 K. Similarly to our interpretation the fans of the Al_3Zr particles which started to form during this thermal treatment were suggested to be responsible for the peak microhardness. The influence of a partial substitution of Zr atoms by V atoms on the microhardness stability was studied in [17]. The isochronal annealing curves (annealing time of 1 hour) exhibited age-hardening starting at about 600 K and the peak values of $HV \cong 100$ were observed at about 700 K. A slight shift of this peak to higher temperatures was found in the V-containing materials. Despite of a very similar volume fraction of strengthening particles, the maximum value of $HV = 120$ observed in the Al-Zr-V alloy annealed at 673 K for 4 hours is more than 20% below the value found in our experiments. The reason for this difference may be found in the fact that a part of V atoms forms relatively coarse particles of the $Al_{10}V$ phase which do not contribute significantly to microhardness and, therefore, the formation of the strengthening $Al_3(Zr,V)$ phase is partially reduced.

The binary Al-Ti alloy does not exhibit any age-hardening response despite of the formation of particles close to the centres of some grains. No fan shaped precipitation was observed, and a large amount of solutes may be located in coarse constitutional particles which do not represent an effective barrier for moving dislocations. The literature data on microhardness of thermally treated binary Al-Ti alloys are missing. The isochronal annealing curve of microhardness (annealing time 1 hour) measured in the melt-spun Al-3.9wt.%Ti-0.34wt.% Si alloy exhibits the maximum of $HV = 90$ in the temperature range between 673 and 773 K [18]. Precipitation of the metastable $L1_2$ modification of the $(Al,Si)_3Ti$ phase was suggested as the reason for the age-hardening response. The expected volume fraction of strengthening particles which are usually concentrated close to the grain centres in this alloy is about 80% higher than in our materials and this difference may explain the higher maximum microhardness value as compared with our Al-Ti alloy. However, the comparison with the Zr-rich Al-Zr-Ti alloys confirms much lower strengthening effect of $L1_2$ Al_3Ti-based particles as compared with the $L1_2$ Al_3Zr-based particles.

Contrary to relatively scarce data on microhardness of rapidly solidified Al-Zr- and Al-Ti-based alloys, numerous investigations were reported on the structure development in these materials during their annealing at elevated temperatures. The general sequence of the decomposition of supersaturated binary Al-Zr alloys is the following [2, 3, 5, 13, 19–22]:

– the formation of the metastable modification of the Al_3Zr phase with cubic $L1_2$ structure either in the form of very fine rod-like particles arranged into fans or in the form of slightly coarser individual spherical particles,

– the formation of the stable modification of the Al_3Zr phase with tetragonal DO_{23} structure in the form of coarse rods or plates.

A great attention was paid to the explanation of the arrangement of $L1_2$ particles into fans. This morphology was found in all published investigations performed in binary Al-Zr alloys. Ryum [19] assumed that segregation of Zr atoms in the supersaturated matrix causes that arms of fans are formed at places with higher concentration of Zr atoms while the spherical particles are formed at places with lower Zr atom concentration. However, this assumption was not verified experimentally. Nes and Billdal introduced a new idea that the fans are formed due to a discontinuous precipitation reaction [21]. This idea was supported by the observation of grain boundary bulging and by the presence of fans inside the grain boundary bulges [3, 5]. Octor and Naka [22] found a significant difference between the precipitation modes occurring in the binary Al-Zr and ternary Al-Cr-Zr alloys. While the discontinuous precipitation resulting in the fan shaped arrangement of Al_3Zr particles occurs in the binary alloy a homogeneous precipitation of very fine Al_3Zr particles was observed in the ternary alloy. It is supposed that other particles (probably of the $Al_{13}Cr_2$ phase in the Al-Cr-Zr alloy) pin the boundaries, thus, suppress the discontinuous precipitation reaction and favour the homogeneous precipitation. Similar phenomenon was observed also in the chill cast Al-Zr alloys containing small amounts of Si and Ti [23]. The presence of Si or Ti suppressed the discontinuous precipitation of the $L1_2$ Al_3Zr-based phase and favoured the continuous formation of spherical modification of this phase. It was suggested that due to a strong binding energy between Si and Ti atoms and vacancies in Al [24] the quenched-in excess vacancies formed clusters with Si and Ti atoms which might act as nucleation sites for the $L1_2$ Al_3Zr-based phase.

The discontinuous type of precipitation was considered unfavourable for the maximum strengthening [23] and, therefore, some attempts were made to avoid the formation of fans and to support the continuous precipitation of spherical particles of the $L1_2$ phase. Numerous investigations were performed in the Al-Zr-V-Ti alloys [25–29] where Zr, Ti and V are believed to be mutually substitutable in the metastable $Al_3(Zr,V,Ti)$ phase. The precipitation mode of this phase was found dependent on the Zr : Ti : V ratio. Chen et al. [26] observed in some ternary Al-Zr-V alloys that Zr-rich alloys exhibited (similarly to the binary Al-Zr alloys) a tendency

to discontinuous precipitation. On the other hand, an increase in V content to V:Zr = 3:1 favoured the continuous precipitation. This result was explained on the assumption that the latter alloy exhibited the minimum lattice mismatch between the $Al_3(Zr,V)$ phase and the Al-based matrix and, therefore, the lowest energy barrier to homogeneous nucleation. Such explanation does not seem to be generally valid as our experiments show that the Al-Zr-Ti alloy with minimum lattice mismatch (stoichiometric parameter $x = 0.75$) exhibits a very intense discontinuous precipitation whereas the alloy with much higher lattice mismatch ($x = 0.25$) exhibits preferentially the continuous precipitation. Another possible reason for the difference in the precipitation mode may be found in a significantly lower diffusion rate of Zr in Al as compared with diffusion rates of V and Ti [30]. The low diffusion rate of Zr favours the discontinuous reaction as it is kinetically faster due to a shorter diffusion path. An increasing content of V or Ti, which substitute for Zr, leads to an acceleration of diffusion rate and supports the continuous reaction.

The continuous precipitation mode in the Al-Zr-V-Ti is usually favoured by the increase in the annealing temperature [25]. Pre-annealing at 773 K for 1 hour was used in [4, 27–29] to suppress discontinuous reaction even in the Zr-rich alloys. Moreover, Chung et al. [29] pointed out that this thermal treatment resulted in a smaller size and lower coarsening rate of spherical particles of the $L1_2$ $Al_3(Zr,V,Ti)$ phase and, consequently, a higher strength should be expected. It was suggested that the pre-annealing reduces the supersaturation of the matrix and slows down the kinetic of the particle growth. However, the way how the supersaturation is reduced was not specified in [29]. Our X-ray diffraction experiments revealed that a considerable volume fraction of the stable modification of the $Al_3(Zr_xTi_{1-x})$ phase was formed during annealing at 773 K for 1 hour. As the size of these particles is considerably larger than that of the metastable $Al_3(Zr_xTi_{1-x})$ phase, we expected (contrary to [29]) a drop in strength resulting from the pre-annealing at 773 K. Microhardness measurements confirmed this expectation and the samples annealed at 773 K for 1 hour were strongly over-aged (Fig. 1). The influence of annealing at high temperatures on the precipitation mode of the metastable $Al_3(Zr,V,Ti)$ phase may be explained by the diffusion rates of solutes which form this phase. According to data of Lee [30] the diffusion rates of Zr, V and Ti at 773 K are much faster than at lower temperatures and nearly equal for all solutes mentioned. Consequently, there is no reason for a different precipitation reaction in alloys containing Zr, V and Ti and the continuous precipitation reaction is favoured.

The decomposition behaviour observed in our Al-Ti alloy is in general accordance with literature data [16, 18]. Discontinuous precipitation mode was not observed in Al-Ti alloys. Formation of particle clusters near the centres of some grains and precipitation free zones along grain boundaries are typical features of decomposition of supersaturated Al-Ti alloys. The composition and crystallography of the metastable phase resulting from the decomposition remain still unclear.

Nie et al. [16] reported that the $L1_2$ Al_3Ti phase formed the particle clusters in grains containing originally coarse primary particles. On the other hand, Pandey et al. [31] did not observe the formation of the $L1_2$ Al_3Ti phase during decomposition. Similar discrepancy was observed also in our Al-Ti alloy. While selected area electron diffraction pointed out that some particle clusters are formed by the $L1_2$ Al_3Ti phase the X-ray diffraction peaks observed incidentally in some annealed samples did not correspond to this structure and were not identified. These results might be explained by the purity of the Al-Ti alloy studied. Other impurities, e.g. Fe and Si, were detected in some particles. Zhang et al. [32] observed similar particle clusters close to the centres of grains in the Al-V alloy containing Fe and microdiffraction patterns obtained from these regions revealed the quasicrystalline character of these particles.

5. Conclusions

1. Isochronal annealing curves of microhardness ($t = 1$ hour) revealed the age hardening response in all Zr-containing Al-Zr-Ti alloys. The maximum value of $HK \cong 150$ was found in all Zr-rich alloys ($x \geq 0.5$) at the annealing temperature close to 650 K. Much lower maximum value of $HK \cong 90$ was observed in the Ti-rich Al-Zr-Ti alloy with $x = 0.25$. This maximum was shifted to the temperature of 700 K. Over-ageing occurs in all Zr-containing Al-Zr-Ti alloys at higher temperatures.

2. Isothermal annealing experiments revealed that a partial substitution of Ti for Zr atoms in the $Al_3(Zr_xTi_{1-x})$ phase improves the microhardness stability at elevated temperatures. No reduction in microhardness of the Al-$Al_3(Zr_{0.5}Ti_{0.5})$ alloy was observed at 600 K for annealing times up to 500 hours.

3. The maximum microhardness of Zr-containing Al-Zr-Ti alloys is achieved in samples with a dense distribution of very fine particles of the $L1_2$ $Al_3(Zr_xTi_{1-x})$ phase arranged into fans. Discontinuous precipitation is the reason for such particle arrangement. This precipitation mode is probably favoured because of very slow diffusion rate of Zr in Al.

4. The onset of over-ageing is clearly connected with the formation of particles of the stable $D0_{23}$ $Al_3(Zr_xTi_{1-x})$ phase. Much larger size of these particles explains the observed decrease in microhardness. Consequently, the pre-annealing at 773 K/1 hour suggested in literature for the suppression of the discontinuous precipitation, does not seem to be a suitable method how to reach the maximum strength.

5. The level of microhardness in the Al-Ti alloy is significantly lower and no age-hardening was observed. Only a slight microhardness decrease was found at the highest annealing temperatures. The poor strength characteristics correspond to the complete absence of discontinuous precipitation. Clusters of particles in some grains and the formation of precipitation free zones are the typical microstructural

features in annealed Al-Ti samples. The nature of cluster forming particles is not yet fully understood.

Acknowledgements

The authors are grateful to Dr. D. Plischke, Crystal Laboratory Göttingen, Germany, for the preparation of thin ribbons. The research was supported by the Grant Agency of the Charles University through the grant No. 283 and by the Grant Agency of the Czech Republic through the grant No. 93-2432. Alexander von Humbolt Foundation has kindly donated the microhardness tester to the Department of Metal Physics of the Charles University, Prague.

REFERENCES

[1] JONES, H.: Mater. Sci. Eng., *5,* 1969/70, p. 1.
[2] SAHIN, E.—JONES, H.: Extended solid solubility, grain refinement and age hardening in Al – 1 to 13 wt. % Zr rapidly quenched from the melt. In: Rapidly Quenched Metals III. Ed.: Cantor, B. London, The Metals Soc. 1978, p. 138.
[3] CHAUDHURY, Z. A.—SURYANARAYANA, C.: Metallography, *17,* 1984, p. 231.
[4] ZEDALIS, M.—FINE, M. E.: Met. Trans. A, *17,* 1986, p. 2187.
[5] PANDEY, S. K.—GANGOPADHYAY, D. K.—SURYANARAYANA, C.: Z. Metallkde, *77,* 1986, p. 12.
[6] MONDOLFO, L.: In: Aluminium Alloys: Structure and Properties. London, Butterworth 1976.
[7] TSUNEKAWA, S.—FINE, M. E.: Scripta Metall., *16,* 1982, p. 391.
[8] ZEDALIS, M. S.—FINE, M. E.: Scripta Metall., *17,* 1983, p. 1247.
[9] LEE, H. M.—LEE, J.—LEE, Z.-H.: Scripta Metall. Mater., *25,* 1991, p. 517.
[10] MÁLEK, P.—BARTUŠKA, P.—PLEŠTIL, J.: Kovove Mater., *37,* 1999, p. 386.
[11] MÁLEK, P.—JANEČEK, M.—SMOLA, B.—BARTUŠKA, P.: Kovove Mater., *38,* 2000, p. 9.
[12] BRAUER, G.: Z. Anorg. Allgem. Chem., *242,* 1939, p. 1.
[13] NES, E.: Acta Metall., *20,* 1972, p. 499.
[14] SRINIVASAN, S.—DESCH, P. B.—SCHWARZ, R. B.: Scripta Metall. Mater., *25,* 1991, p. 2513.
[15] MÁLEK, P.—CHALUPA, B.—PLEŠTIL, J.: Kovove Mater., *38,* 2000, p. 77.
[16] NIE, J. E.—MAJUMDAR, A.—MUDDLE, B. C.: Mater. Sci. Eng. A, *179/180,* 1994, p. 619.
[17] PARK, W.-W.—KIM, T.-H.: Scripta Metall., *22,* 1988, p. 1709.
[18] YOU, B.-S.—PARK, W.-W.: Scripta Mater., *34,* 1996, p. 201.
[19] RYUM, N.: Acta Metall., *17,* 1969, p. 269.
[20] IZUMI, O.—OELSCHLÄGEL, D.: Scripta Metall., *3,* 1969, p. 619.
[21] NES, E.—BILLDAL, H.: Acta Metall., *25,* 1977, p. 1039.
[22] OCTOR, H.—NAKA, S.: Phil. Mag. Letters, *59,* 1989, p. 229.
[23] SATO, T.—KAMIO, A.—LORIMER, G. W.: Mater. Sci. Forum, *217-222,* 1996, p. 895.
[24] PERRY, A. J.—ENTWITSLE, E. M.: Phil. Mag., *18,* 1968, p. 1085.
[25] CHEN, I. C.—FINE, M. E.—WEERTMAN, J. R.—LEWIS, R. E.: Scripta Metall., *21,* 1987, p. 1003.
[26] CHEN, I. C.—FINE, M. E.—WEERTMAN, J. R.: Acta Metall. Mater., *38,* 1990, p. 771.

[27] PARAMESWARAN, W. R.—WEERTMAN, J. R.—FINE, M. E.: Scripta Metall., *23*, 1989, p. 147.
[28] LEE, H.—HAN, S. Z.—LEE, M. H.—LEE, Z.-H.: Mater. Sci. Eng. A, *163*, 1993, p. 81.
[29] CHUNG, S. C.—HAN, S. Z.—LEE, H. M.—KWON, H.-S.: Scripta Metall. Mater., *33*, 1995, p. 687.
[30] LEE, H. M.: Scripta Metall. Mater., *24*, 1990, p. 2443.
[31] PANDEY, S. K.—SURYANARAYANA, C.: Mater. Sci. Eng. A, *111*, 1989, p. 181.
[32] ZHANG, X. D.—BI, Y. J.—LORETTO, M. H.: Acta Metall. Mater., *41*, 1993, p. 849.

Received: 19.4.1999